Science Advances
AAAS

Supplementary Materials for

Foxq2 determines blue cone identity in zebrafish

Yohey Ogawa, Tomoya Shiraki, Yoshitaka Fukada*, Daisuke Kojima*

*Corresponding author. Email: sfukada@mail.ecc.u-tokyo.ac.jp (Y.F.);
sdkojima@mail.ecc.u-tokyo.ac.jp (D.K.)

Published day month 2021, *Sci. Adv.* **7**, eabi9784 (2021)
DOI: 10.1126/sciadv.abi9784

The PDF file includes:

Other Supplementary Material for this manuscript includes the following:

Supplementary Text

FOXQ2 gene has not been annotated in the genome of platypus, which is the closest relatives to humans among the vertebrate species having *SWS2* gene (*33*). As observed in zebrafish (Fig. 4A-C and S5), platypus *FOXQ2* is presumably expressed only in the retina (only in SWS2 cones), and the tissue-specific and low-level expression of the transcription factor could be one of the reasons why *FOXQ2* has not been identified to date in the platypus genome. We examined whether platypus genome contains *FOXQ2* gene, with special attention to the forkhead domain (a DNA-binding domain) highly conserved among FOXQ2 subfamily members (Fig. 7A). A tblastn-guided searching and subsequent manual annotation identified a genomic region showing the highest alignment score against the amino acid sequence of the forkhead domain of zebrafish Foxq2 (Fig. 7A). In the phylogenetic tree based on the amino acid sequences of the forkhead domain, the platypus sequence is clustered into FoxQ2 subfamily composed of vertebrate and invertebrate members (Fig. S8). We also identified a previously unannotated *FOXQ2* sequence in the genome of chicken (Fig. 7), which has been widely studied as a model species having SWS2 cone subtype (*65*). These lines of genomic evidence suggest that the FOXQ2-SWS2 axis is evolutionarily conserved among vertebrate species.

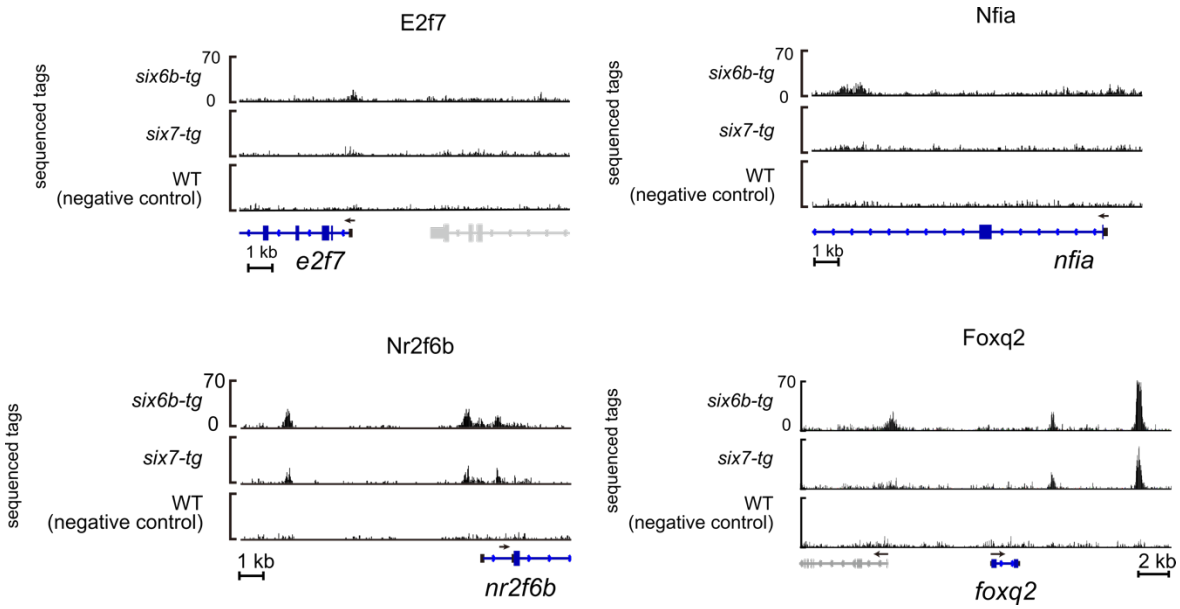

Fig. S1.

DNA-binding of Six6b and Six7. Visualization of Six6b and Six7 ChIP-seq peaks obtained from the adult retina of *six6b-tg* (ja70Tg), *six7-tg* (ja69Tg), and wild-type zebrafish with anti-FLAG antibody. The ChIP-seq data were retrieved from our previous paper (*20*). The direction of transcription is indicated by an arrow. 5'-UTRs and coding exons are represented in black and blue boxes, respectively.

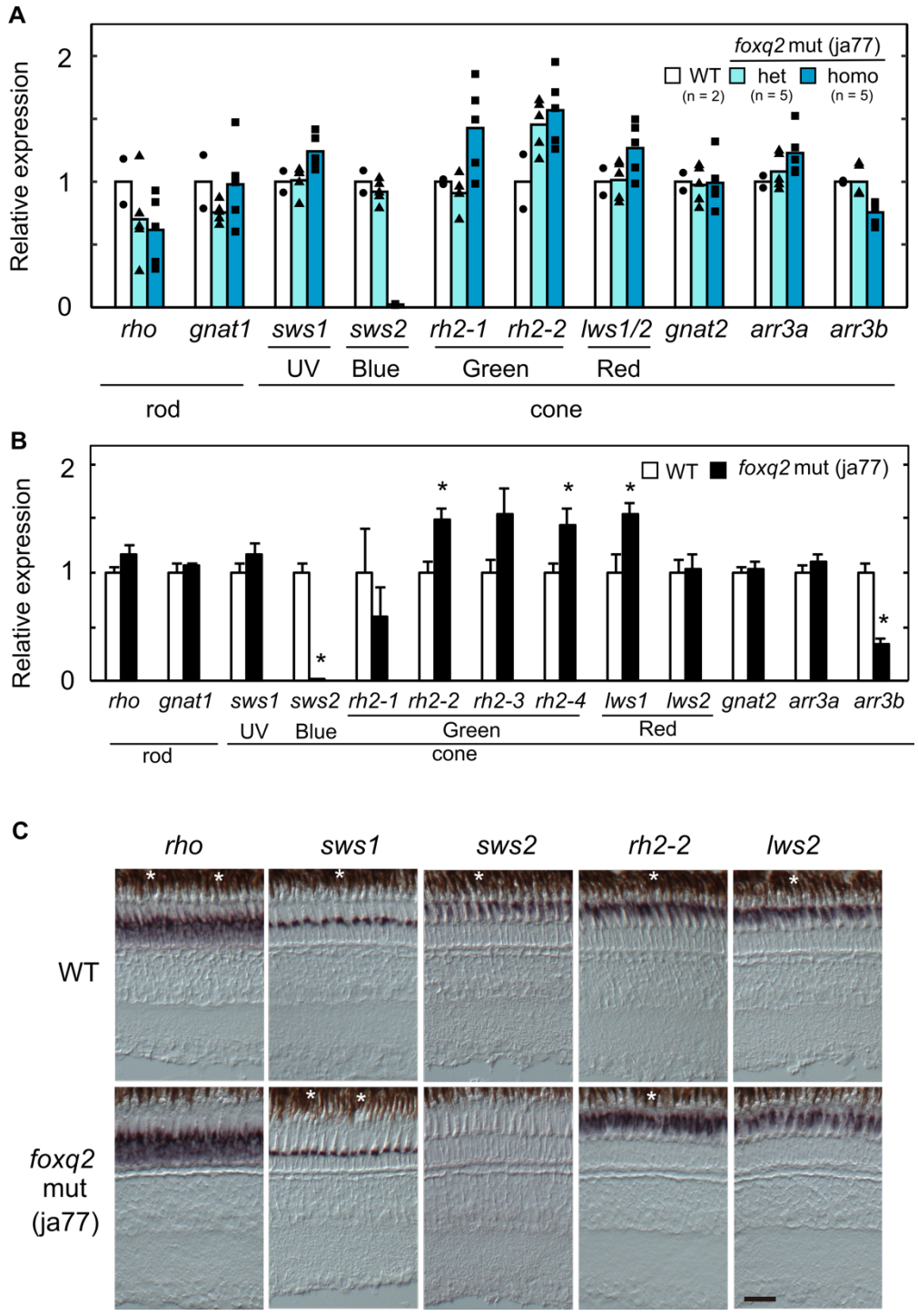

Fig. S2.

Analysis of another line of *foxq2* mutant zebrafish (A) Related to Fig. 1C and Fig.1D. Expression profiles of phototransduction genes in the 5-dpf larval eyes of *foxq2* mutant (ja77). Mean values of expression levels for each genotype are indicated as bars, while individual values are shown as markers with distinct shape among three genotypes. The number of fish used is

presented in the graph legend. **(B)** Expression profiles of phototransduction genes in the adult eyes of *foxq2* mutant (ja77). Mean ± SEM (n = 5). *P < 0.05 by Student's t-test. **(C)** Expression patterns of rod and cone opsin genes examined by *in situ* hybridization using the adult eyes of *foxq2* mutant (ja77). The retinal pigmented epithelium (RPE, indicated by asterisks) is adjacent to the photoreceptor layer. Scale bar, 50 μm.

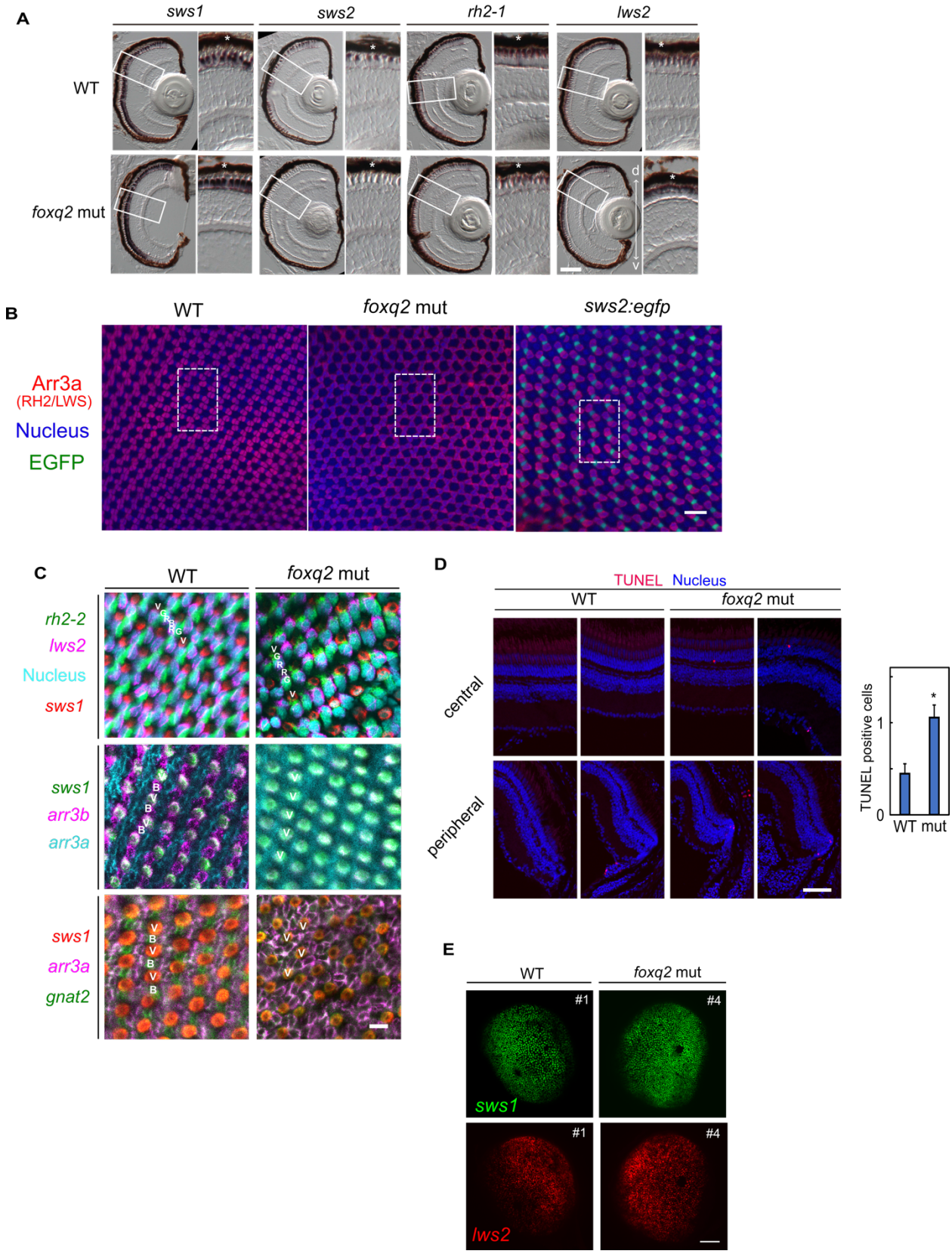
A
sws1
sws2
rh2-1
lws2
WT
foxq2 mut
d
v
B
WT
foxq2 mut
sws2:egfp
Arr3a
(RH2/LWS)
Nucleus
EGFP
C
WT
foxq2 mut
rh2-2
lws2
Nucleus
sws1
sws1
arr3b
arr3a
sws1
arr3a
gnat2
D
TUNEL Nucleus
WT
foxq2 mut
central
peripheral
TUNEL positive cells
1
0
WT mut
E
WT
foxq2 mut
#1
#4
sws1
#1
#4
lws2

Fig. S3.

Expression pattern of phototransduction genes in *foxq2* mutant zebrafish **(A)** Expression pattern of cone opsin genes examined by *in situ* hybridization using 5-dpf larval eyes of the *foxq2* mut (ja74). Magnified view (a box surrounded with white lines) is indicated in the right side of each panel. The retinal pigmented epithelium (RPE, indicated by asterisks) is adjacent to the photoreceptor layer. d-v, dorsal-ventral retina. Scale bar, 50 μm. **(B)** Related to Fig. 2B. Fluorescent images of the flat-mounted retinas prepared from the adult WT, the *foxq2* mut (ja74), and *Tg(-3.5opn1sw2:EGFP)*^{kj11Tg} (*sws2:egfp*). V: SWS1 cone, B: SWS2 cone, G: RH2 cone, R: LWS cone. The retinas were immunostained with zpr1 antibody to detect a RH2 and LWS cone-specific phototransduction protein (*arr3a*, red) and also stained with DRAQ5 to highlight cell nuclei. Scale bar, 20 μm. **(C)** Related to Fig. 2C. Fluorescent images of the flat-mounted retinas prepared from the adult WT and the *foxq2* mut (ja74). Expression of cone opsin genes and cone-type phototransduction gene were visualized by *in situ* HCR. V: SWS1 cone, B: SWS2 cone, G: RH2 cone, R: LWS cone. Scale bar, 10 μm. **(D)** Related to Fig. 2D. **(**Left) Fluorescent images in retinal cryosections from the adult fish labeled for TUNEL (red). The cell nuclei were counterstained with DAPI (blue). Scale bar: 50 μm. (Right) Quantification of TUNEL-positive cells in the central and peripheral retina. The numbers of TUNEL-positive cells were counted for each cryosection and averaged (mean ± SEM, $n = 56$ for WT, $n = 72$ for the *foxq2* mut; $*P < 0.05$, Student's t test). The TUNEL staining was independently conducted from that in Fig. 2D with distinct individual fish for each experiment. **(E)** Related to Fig. 2E. Expression pattern of *sws1* and *lws2* examined by *in situ* HCR using 5-dpf larval eyes of the *foxq2* mut (ja74). The number in the upper-right corner for each panel represents the unique identity of the eye. Scale bar, 50 μm.

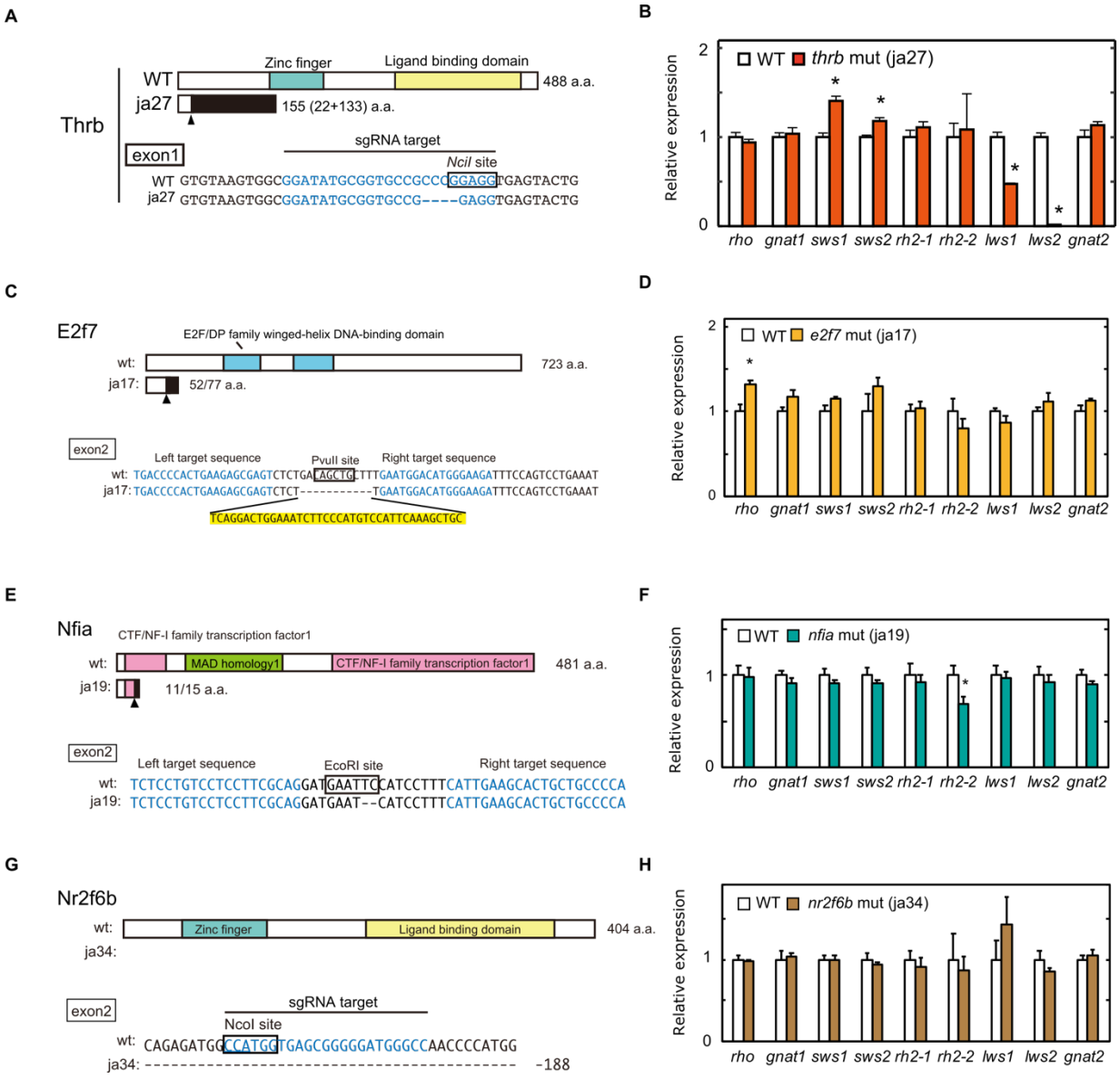

Fig. S4.

Analysis of cone-enriched gene mutants (A, C, E, G) Schematic representation of Thrb, E2f7, Nfia and Nr2f6b, and their partial nucleotide sequences. Frameshift site is indicated by an arrowhead. Nucleotide deletions are indicated by dashes. Nucleotide insertion is highlighted in yellow. The nucleotide sequences highlighted in blue indicate the target sequences of TAL-effector nucleases or Cas9-sgRNA complexes. The recognition sites of the restriction endonucleases, *Nci*I, *Pvu*II, *EcoR*I, and *Nco*I are surrounded by black lines. The ja27 mutation (4-bp loss) caused a frame shift of the amino acid sequence of Thrb2, which is an isoform of Thrb and essential for LWS opsin expression in mice and zebrafish (*13*, *14*). The ja17 mutation caused a frame shift of the amino acid sequence of E2f7 by a combination of 11 bp deletion and 38 bp insertion. The ja19 mutation caused a frame shift of the amino acid sequence of Nfia by 2 bp loss. The ja34 mutation impairs protein translation of Nr2f6b by 188 bp nucleotide deletion

including the ATG initiation site. **(B, D, F, H)** Expression profiles of phototransduction genes in the larval eyes at 5 dpf. Mean ± SEM. *$P < 0.05$ by Student's *t*-test. The number of fish used is as follows: $n = 3$ (*thrb* WT), $n = 4$ (*thrb* mut); $n = 4$ (*e2f7* WT), $n = 4$ (*e2f7* mut); $n = 3$ (*nfia* WT), $n = 4$ (*nfia* mut); $n = 4$ (*nr2f6b* WT), $n = 4$ (*nr2f6b* mut). The expression levels of *sws2* and *rh2* genes are reproduced in the Fig. 1B.

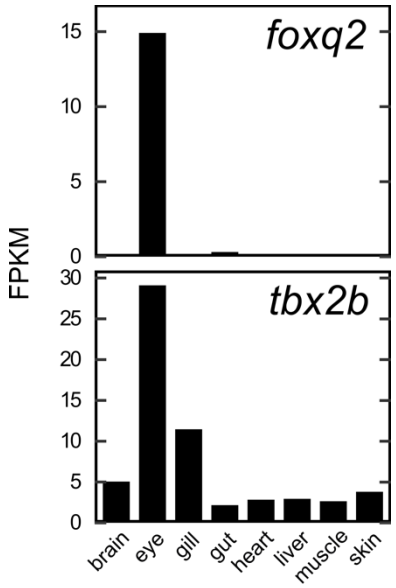

Fig. S5.

Transcript levels of *tbx2b* and *foxq2* in zebrafish adult tissues

Related to Fig. 4A. FPKM (fragment per kilobase per million) values were retrieved from the previous study (*66*).

Fig. S6.

Nucleotide sequence of zebrafish *sws2* promoter. The translational start site is indicated as +1. DNA-binding motifs of Fox and Crx transcription factors were predicted by our motif scanning analysis and are highlighted as follows: FkhP motif (RYAAAYA) in *green*, FkhS motif (AHAACA) in *blue*, and Crx motif (TAATCY) in *yellow*.

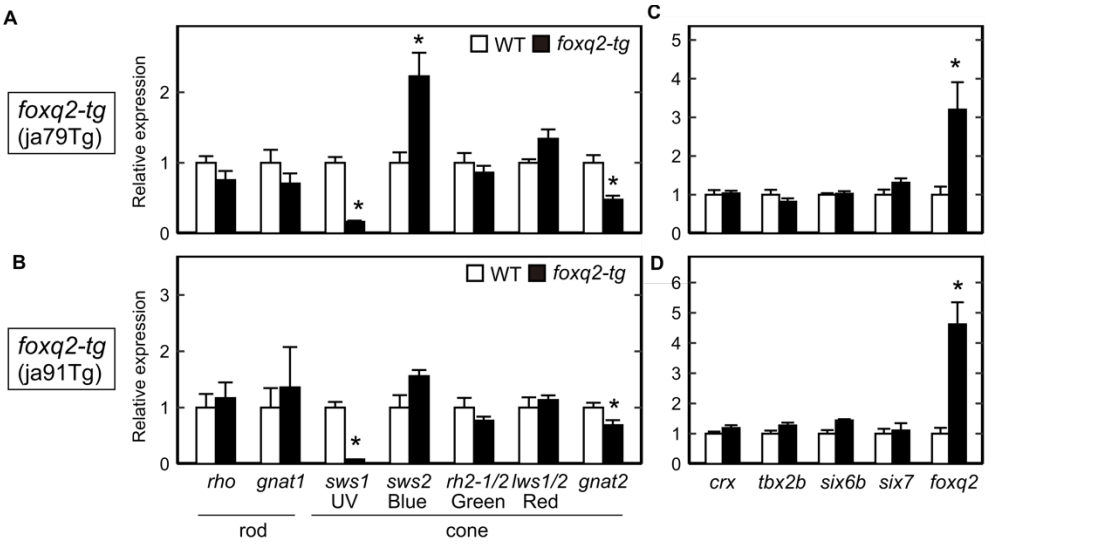
A
foxq2-tg
(ja79Tg)
Relative expression
WT
foxq2-tg
B
foxq2-tg
(ja91Tg)
rho
gnat1
sws1
UV
sws2
Blue
rh2-1/2
Green
lws1/2
Red
gnat2
rod
cone
C
crx
tbx2b
six6b
six7
foxq2
D

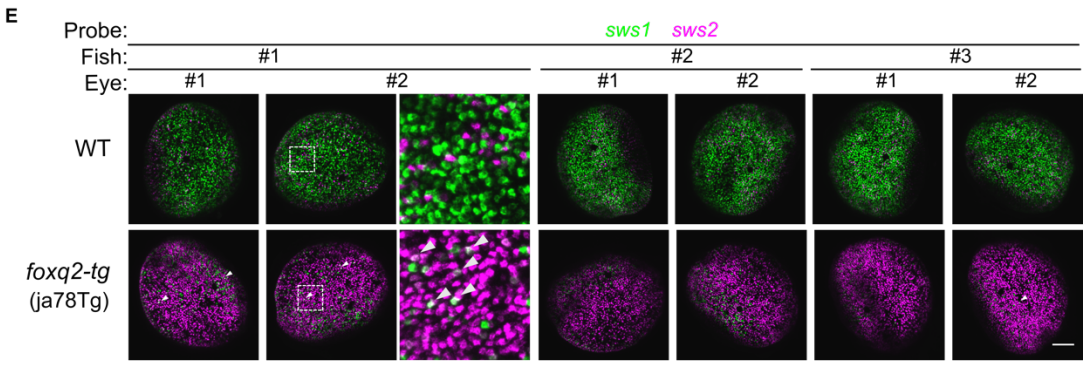
E
Probe:
sws1 sws2
Fish:
#1
#2
#3
Eye:
WT
foxq2-tg
(ja78Tg)

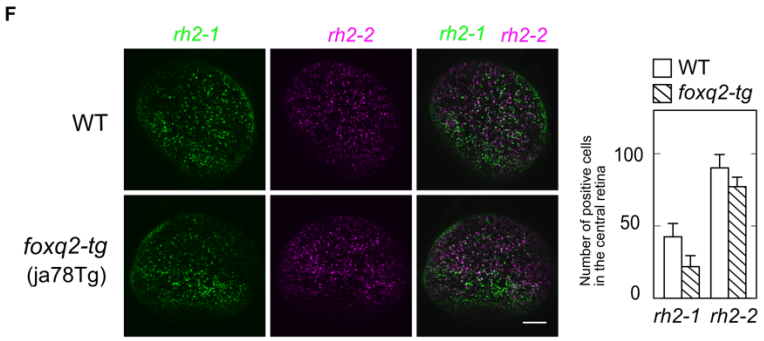
F
rh2-1
rh2-2
rh2-1 rh2-2
WT
foxq2-tg
(ja78Tg)
WT
foxq2-tg
Number of positive cells
in the central retina
100
50
0
rh2-1 rh2-2

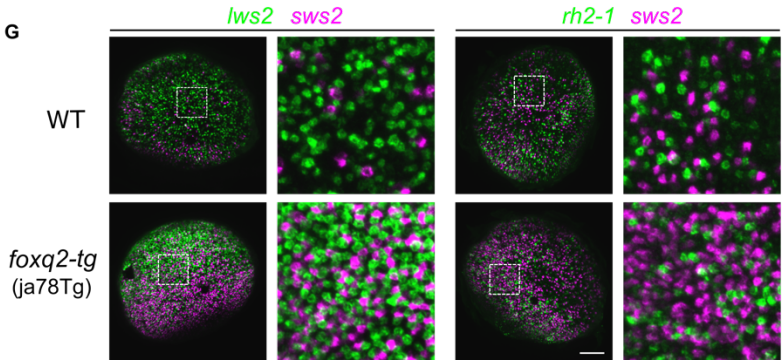
G
lws2 sws2
rh2-1 sws2
WT
foxq2-tg
(ja78Tg)

Fig. S7.

Expression analyses of *foxq2-tg* transgenic zebrafish lines. (A-D) Related to Fig. 6C and 6D. Expression profiles of phototransduction genes (A and B) and transcription factors (C and D) in the 5 dpf-larval eyes of the *foxq2-tg* (ja79Tg and ja91Tg). Mean ± SEM (n = 4). *P < 0.05 by Student's t-test. **(E)** Related to Fig. 6E and 6F. Fluorescent images used for quantification of the number of *sws1*- and *sws2*-positive cells. Magnified view (a box surrounded with white broken lines) is indicated in the right side of the panel. *sws1* and *sws2* are expressed in different cells in the wild-type, while some *sws1* expression signals are colocalized with those of *sws2* (arrowheads). Scale bar, 50 μm. **(F)** Expression pattern of *rh2-1* and *rh2-2* examined by *in situ* HCR using 5-dpf larval eyes of the *foxq2-tg* (ja78Tg). The number of opsin gene-positive cells in the central region of the retina is indicated in a bar graph. Data are represented by Mean ± SEM (n = 6). Statistical significance between two genotype was determined by Student's t-test (*P < 0.05). Scale bar, 50 μm. **(G)** Related to Fig. 6F. Expression pattern of *sws2, rh2-2,* and *lws2* examined by *in situ* HCR using 5-dpf larval eyes of the *foxq2-tg* (ja78Tg). Magnified view (a box surrounded with white broken lines) is indicated in the right side of each panel. Scale bar, 50 μm.

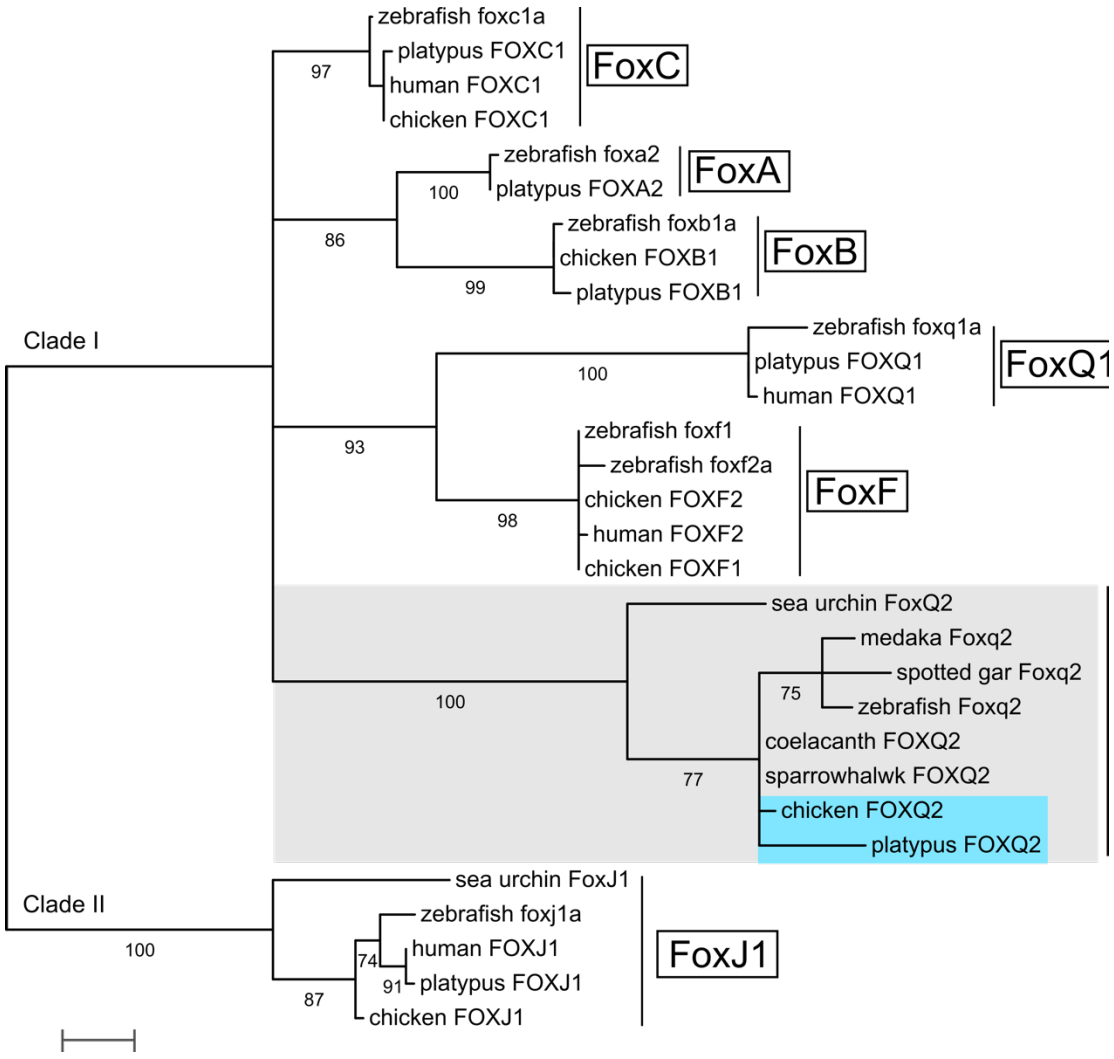

Fig. S8.

Phylogenetic analysis of *FOX* genes. A Maximum-likelihood tree constructed from amino acid sequences of the forkhead domain with 500 bootstrapping replications. Numerical values indicating bootstrap support are shown at the base of each node. The scale bar indicates 0.1 substitutions per site. Accession numbers and their sequences used for tree construction are listed in Dataset S4. Branches with bootstrap value below 70% are collapsed. FOXA, FOXB, FOXC, FOXF, and FOXQ are categorized into Clade I, while FOXJ is categorized into Clade II.

Table S1. Zebrafish lines used for this study

Genotype	Genomic Feature	Figure	Reference
tbx2b	ja20	1, 4	This study
thrb	ja27	1, S4	This study
nr2f6b	ja34	1, S4	This study
e2f7	ja17	1, S4	This study
nfia	ja19	1, S4	This study
foxq2	ja74	1, 2, 4, S3	This study
foxq2	ja77	S2	This study
six6a	ja62	4	(*20*)
six6b	ja63	4	(*20*)
six7	ja51	4, 6	(*17*)
Tg(rho:egfp)	ja2Tg	1	(*46*)
Tg(gnat2:egfp)	ja23Tg	1	(*17*)
Tg(-5.5opn1sw1:EGFP),	kj9Tg	3	(*48*)
Tg(-3.5opn1sw2:EGFP)	kj11Tg	3	(*31*)
Tg(opn1mw2:EGFP)	kj4Tg	3	(*49*)
Tg(-0.6opn1lw1-lws2:GFP)	kj19Tg	3	(*50*)
Tg(-5.2crx:EGFP-2A-FLAG-foxq2)	ja78Tg	6, S7	This study
Tg(-5.2crx:EGFP-2A-FLAG-foxq2)	ja79Tg	S7	This study
Tg(-5.2crx:EGFP-2A-FLAG-foxq2)	ja91Tg	S7	This study

Table S2. Target sequences of TALENs and gRNA

Target gene	Target Sequence	target exon
foxq2	GGCTGGAAGAGCAGAACCAG	Exon1
foxq2	GGAAGTCTTGAAAGTTGGCC	Exon2
thrb	GGATATGCGGTGCCGCCCGG	Exon1
nr2f6	GGCCCATCCCCCGCTCACCA	Exon2
tbx2b	TATTGTGAGAGCCAACGAT (left) TATGTCCTGAAAGTGCTGT (right)	Exon3
e2f7	TGACCCCACTGAAGAGCGAGT (left) TCTTCCCATGTCCATTC (right)	Exon2
nfia	TCTCCTGTCCTCCTTCGCAG (left) TGGGGCAGCAGTGCTTCAATG (right)	Exon2

Table S3. Primers used for genotyping PCR

Target	Forward (5' to 3')	Reverse (5' to 3')	Amplicon Length (bp)	Restriction enzyme
foxq2_exon1 (HRMA)	CAGCAATCGAGAAC AACTTGGAC	TCACTGTCCTGT TCTGAG	168	
foxq2_exon2 (HRMA)	GGAGAAACAGCGTC AGACACAA	TGTTACCCTGCG GATCCTTCTC	170	
foxq2_ja77	AAACTTTTGACCTTT ATAGGAGTC	CCAGCTCCAGTA GACTCTAGG	359	*Hae*III
thrb	TGTAAGCACGTCAAC GTGATCG	ACCTTTCTTATG TGGCCCTTGC	470	*Nci*I
nr2f6b	CTTCAGAGTGCTGTT AAACGTG	AACAGCGTGTG ATTGGCTGTTG	541	*Nco*I
tbx2b	GTCCGCATGACTGGT TTGTTTC	CACCAAATGTA CAGGCTCGTAG	499	*Hind*III
e2f7	AGGATTTGCTTGGTG TCAGAAC	TCTACCTGACAC GAGTCATC	460	*Pvu*II
nfia	CTGGCCGAAATGTAA CAAAGAC	ACAAAATCCTC GCGGAACTC	523	*Eco*RI

Table S4. Primers used for quantitative PCR.

Target gene	Forward (5' to 3')	Reverse (5' to 3')
crx	CATAACTGGAGGGGAATCTG	AAAGCACGACACAAGAACTC
tbx2b	CGACTCTGATGCTTCCTCAAG	GTCCATTTCGTGCTCGCTATC
six6b	CGCAAAAAACAGGTTACAAC	ATTCCCCAGTCGGTCTACAG
six7	CTGCAGGACCCTTATCCAAAC	CATTCAGGAGAACTTCCAGAC
thrb	AACTTGGACGATTCAGAGGTG	TGAGCCACCTTGTGCTTACG
*thrb2**	CTCAGTCACTATCACCAACAAG	TGTCTCCACAAACAACACAC
foxq2	CAGTCCTACATTGCCCTCATTTC	GATTGTGTCTGACGCTGTTTCTC

*Thrb isoform: ENSDART00000189391.1.

Table S5. Combinations of Alexa fluor-conjugated hairpins and probe sets used for *in situ* HCR

Figure	B1 hairpins		B3 hairpins		B5 hairpins	
	Probeset	Alexa-Fluor	Probeset	Alexa-Fluor	Probeset	Alexa-Fluor
Figure 2A	arr3a	488	arr3b	647	sws1	546
Figure 2C	rh2-2cds	488	lws2	647	sws1	546
Figure 2C	arr3a	488	gnat2	647	sws1	546
Figure 2E	sws2	647	lws2	488	sws1	546
Figure 2E	rh2-2UTR	647	gnat2	488	rh2-1UTR	546
Figure 3D	sws2	546	foxq2	647		
Figure 3E	arr3a	488	foxq2	647	sws1	546
Figure 4C	sws2	546	foxq2	647		
Figure 6E	sws2	647			sws1	546
Figure 6F	sws2	647			sws1	546
Figure 6F	sws2	647	lws2	546		
Figure 6F	sws2	647			rh2-1UTR	546
Figure S3C	rh2-2cds	488	lws2	647	sws1	546
Figure S3C	arr3a	488	arr3b	647	sws1	546
Figure S3C	arr3a	488	gnat2	647	sws1	546
Figure S3E	sws2	647	lws2	488	sws1	546
Figure S7E	sws2	647			sws1	546
Figure S7F	rh2-2UTR	647			rh2-1UTR	546
Figure S7G	sws2	647	lws2	546		
Figure S7G	sws2	647			rh2-1UTR	546

Table S6. Genomic locations of *FOXQ2* gene used for synteny analysis

Species		assembly	Chromosome/contig
coelacanth	*Latimeria chalumnae*	LatCha1	Scaffold JH127062.1
spotted gar	*Lepisosteus oculatus*	LepOcu1	LG19
zebrafish	*Danio rerio*	GRCz11	chr 22
Medaka	*Oryzias latipes*	ASM223467v1	Primary assembly 4
Sparrowhawk	*Accipiter nisus*	Accipiter_nisus_ver1.0	Primary assembly BJBX01009521.1
Chicken	*Gallus gallus*	GRCg6a	chr 28
Platypus	*Ornithorhynchus anatinus*	mOrnAna1.p.v1	Primary assembly X2
Human	*Homo sapiens*	GRCh38.p13	chr 19

Data S1.

Cone- and rod-enriched genes identified by microarray analysis. Probes whose signal intensities 10-fold higher in cone compared with rod (cone-enriched) and 4-fold higher in rod compared with cone (rod-enriched) are listed in this dataset.

Data S2.

Probe sequences used for *in situ* hybridization chain reaction

Data S3.

Results of motif scanning analysis. Unique IDs of transcription factor motifs in the JASPAR database are included in this dataset.

Data S4.

Nucleotide and amino acid sequences used for inferring phylogenetic tree. The nucleotide sequences of *FOXQ2* genes, identified by blast searching and manual annotation in this study, are indicated by upper case letters for exons, while those are indicated by lower case letters for introns.

REFERENCES AND NOTES

1. T. D. Lamb, Evolution of phototransduction, vertebrate photoreceptors and retina. *Prog. Retin. Eye Res.* **36**, 52–119 (2013).

2. T. H. Goldsmith, Optimization, constraint, and history in the evolution of eyes. *Q. Rev. Biol.* **65**, 281–322 (1990).

3. T. Baden, D. Osorio, The retinal basis of vertebrate color vision. *Annu. Rev. Vis. Sci.* **5**, 177–200 (2019).

4. T. Okano, D. Kojima, Y. Fukada, Y. Shichida, T. Yoshizawa, Primary structures of chicken cone visual pigments: Vertebrate rhodopsins have evolved out of cone visual pigments. *Proc. Natl. Acad. Sci. U.S.A.* **89**, 5932–5936 (1992).

5. S. Yokoyama, Evolution of dim-light and color vision pigments. *Annu. Rev. Genomics Hum. Genet.* **9**, 259–282 (2008).

6. S. P. Collin, M. A. Knight, W. L. Davies, I. C. Potter, D. M. Hunt, A. E. O. Trezise, Ancient colour vision: Multiple opsin genes in the ancestral vertebrates. *Curr. Biol.* **13**, R864–R865 (2003).

7. W. I. L. Davies, S. P. Collin, D. M. Hunt, Molecular ecology and adaptation of visual photopigments in craniates. *Mol. Ecol.* **21**, 3121–3158 (2012).

8. A. Swaroop, D. Kim, D. Forrest, Transcriptional regulation of photoreceptor development and homeostasis in the mammalian retina. *Nat. Rev. Neurosci.* **11**, 563–576 (2010).

9. C. Cepko, Intrinsically different retinal progenitor cells produce specific types of progeny. *Nat. Rev. Neurosci.* **15**, 615–627 (2014).

10. T. Furukawa, E. M. Morrow, C. L. Cepko, Crx, a novel otx-like homeobox gene, shows photoreceptor-specific expression and regulates photoreceptor differentiation. *Cell* **91**, 531–541 (1997).

11. A. J. Mears, M. Kondo, P. K. Swain, Y. Takada, R. A. Bush, T. L. Saunders, P. A. Sieving, A. Swaroop, Nrl is required for rod photoreceptor development. *Nat. Genet.* **29**, 447–452 (2001).

12. N. B. Haider, J. K. Naggert, P. M. Nishina, Excess cone cell proliferation due to lack of a functional NR2E3 causes retinal dysplasia and degeneration in rd7/rd7 mice. *Hum. Mol. Genet.* **10**, 1619–1626 (2001).

13. L. Ng, J. B. Hurley, B. Dierks, M. Srinivas, C. Saltó, B. Vennström, T. A. Reh, D. Forrest, A thyroid hormone receptor that is required for the development of green cone photoreceptors. *Nat. Genet.* **27**, 94–98 (2001).

14. S. C. Suzuki, A. Bleckert, P. R. Williams, M. Takechi, S. Kawamura, R. O. L. Wong, Cone photoreceptor types in zebrafish are generated by symmetric terminal divisions of dedicated precursors. *Proc. Natl. Acad. Sci. U.S.A.* **110**, 15109–15114 (2013).

15. K. C. Eldred, S. E. Hadyniak, K. A. Hussey, B. Brenerman, P.-W. Zhang, X. Chamling, V. M. Sluch, D. S. Welsbie, S. Hattar, J. Taylor, K. Wahlin, D. J. Zack, R. J. Johnston Jr., Thyroid hormone signaling specifies cone subtypes in human retinal organoids. *Science* **362**, eaau6348 (2018).

16. K. Alvarez-Delfin, A. C. Morris, C. D. Snelson, J. T. Gamse, T. Gupta, F. L. Marlow, M. C. Mullins, H. A. Burgess, M. Granato, J. M. Fadool, Tbx2b is required for ultraviolet photoreceptor cell specification during zebrafish retinal development. *Proc. Natl. Acad. Sci. U.S.A.* **106**, 2023–2028 (2009).

17. Y. Ogawa, T. Shiraki, D. Kojima, Y. Fukada, Homeobox transcription factor Six7 governs expression of green opsin genes in zebrafish. *Proc. Biol. Sci.* **282**, 20150659 (2015).

18. A. Chinen, T. Hamaoka, Y. Yamada, S. Kawamura, Gene duplication and spectral diversification of cone visual pigments of zebrafish. *Genetics* **163**, 663–675 (2003).

19. M. Takechi, S. Kawamura, Temporal and spatial changes in the expression pattern of multiple red and green subtype opsin genes during zebrafish development. *J. Exp. Biol.* **208**, 1337–1345 (2005).

20. Y. Ogawa, T. Shiraki, Y. Asano, A. Muto, K. Kawakami, Y. Suzuki, D. Kojima, Y. Fukada, Six6 and Six7 coordinately regulate expression of middle-wavelength opsins in zebrafish. *Proc. Natl. Acad. Sci. U.S.A.* **116**, 4651–4660 (2019).

21. S. L. Renninger, M. Gesemann, S. C. F. Neuhauss, Cone arrestin confers cone vision of high temporal resolution in zebrafish larvae. *Eur. J. Neurosci.* **33**, 658–667 (2011).

22. P. A. Raymond, L. K. Barthel, A moving wave patterns the cone photoreceptor mosaic array in the zebrafish retina. *Int. J. Dev. Biol.* **48**, 935–945 (2004).

23. C. W. Müller, B. G. Herrmann, Crystallographic structure of the T domain-DNA complex of the Brachyury transcription factor. *Nature* **389**, 884–888 (1997).

24. C. D. Snelson, K. Santhakumar, M. E. Halpern, J. T. Gamse, Tbx2b is required for the development of the parapineal organ. *Development* **135**, 1693–1702 (2008).

25. L. I. Volkov, J. S. Kim-Han, L. M. Saunders, D. Poria, A. E. O. Hughes, V. J. Kefalov, D. M. Parichy, J. C. Corbo, Thyroid hormone receptors mediate two distinct mechanisms of long-wavelength vision. *Proc. Natl. Acad. Sci. U.S.A.* **117**, 15262–15269 (2020).

26. P. A. Raymond, L. K. Barthel, R. L. Bernardos, J. J. Perkowski, Molecular characterization of retinal stem cells and their niches in adult zebrafish. *BMC Dev. Biol.* **6**, 36 (2006).

27. J. M. Gross, J. E. Dowling, Tbx2b is essential for neuronal differentiation along the dorsal/ventral axis of the zebrafish retina. *Proc. Natl. Acad. Sci. U.S.A.* **102**, 4371–4376 (2005).

28. K. L. Clark, E. D. Halay, E. Lai, S. K. Burley, Co-crystal structure of the HNF-3/fork head DNA-recognition motif resembles histone H5. *Nature* **364**, 412–420 (1993).

29. C. Larroux, G. N. Luke, P. Koopman, D. S. Rokhsar, S. M. Shimeld, B. M. Degnan, Genesis and expansion of metazoan transcription factor gene classes. *Mol. Biol. Evol.* **25**, 980–996 (2008).

30. S. Nakagawa, S. S. Gisselbrecht, J. M. Rogers, D. L. Hartl, M. L. Bulyk, DNA-binding specificity changes in the evolution of forkhead transcription factors. *Proc. Natl. Acad. Sci. U.S.A.* **110**, 12349–12354 (2013).

31. M. Takechi, S. Seno, S. Kawamura, Identification of cis-acting elements repressing blue opsin expression in zebrafish UV cones and pineal cells. *J. Biol. Chem.* **283**, 31625–31632 (2008).

32. R. R. Beerli, D. J. Segal, B. Dreier, C. F. Barbas, Toward controlling gene expression at will: Specific regulation of the erbB-2/HER-2 promoter by using polydactyl zinc finger proteins constructed from modular building blocks. *Proc. Natl. Acad. Sci. U.S.A.* **95**, 14628–14633 (1998).

33. W. L. Davies, L. S. Carvalho, J. A. Cowing, L. D. Beazley, D. M. Hunt, C. A. Arrese, Visual pigments of the platypus: A novel route to mammalian colour vision. *Curr. Biol.* **17**, R161–R163 (2007).

34. J. K. Bowmaker, Evolution of vertebrate visual pigments. *Vision Res.* **48**, 2022–2041 (2008).

35. G. H. Jacobs, Evolution of colour vision in mammals. *Philos. Trans. R. Soc. B Biol. Sci.* **364**, 2957–2967 (2009).

36. T. W. Cronin, M. J. Bok, Photoreception and vision in the ultraviolet. *J. Exp. Biol.* **219**, 2790–2801 (2016).

37. T. Yoshimatsu, P. Bartel, C. Schröder, F. K. Janiak, F. St-Pierre, P. Berens, T. Baden, Ancestral circuits for vertebrate colour vision emerge at the first retinal synapse. *bioRxiv*, 2020.10.26.356089 (2021).

38. O. Hobert, Regulatory logic of neuronal diversity: Terminal selector genes and selector motifs. *Proc. Natl. Acad. Sci. U.S.A.* **105**, 20067–20071 (2008).

39. Y. Liu, Y. Shen, J. S. Rest, P. A. Raymond, D. J. Zack, Isolation and characterization of a zebrafish homologue of the cone rod homeobox gene. *Invest. Ophthalmol. Vis. Sci.* **42**, 481–487 (2001).

40. T. Ebrey, Y. Koutalos, Vertebrate photoreceptors. *Prog. Retin. Eye Res.* **20**, 49–94 (2001).

41. J. H. Fritzenwanker, J. Gerhart, R. M. Freeman Jr., C. J. Lowe, The Fox/Forkhead transcription factor family of the hemichordate *Saccoglossus kowalevskii*. *EvoDevo* **5**, 17 (2014).

42. C. Sinigaglia, H. Busengdal, L. Leclère, U. Technau, F. Rentzsch, The bilaterian head patterning gene six3/6 controls aboral domain development in a cnidarian. *PLoS Biol.* **11**, e1001488 (2013).

43. R. C. Range, Z. Wei, An anterior signaling center patterns and sizes the anterior neuroectoderm of the sea urchin embryo. *Development* **143**, 1523–1533 (2016).

44. T. D. Lamb, S. P. Collin, E. N. Pugh Jr., Evolution of the vertebrate eye: Opsins, photoreceptors, retina and eye cup. *Nat. Rev. Neurosci.* **8**, 960–976 (2007).

45. D. Arendt, K. Tessmar-Raible, H. Snyman, A. W. Dorresteijn, J. Wittbrodf, Ciliary photoreceptors with a vertebrate-type opsin in an invertebrate brain. *Science* **306**, 869–871 (2004).

46. Y. Asaoka, H. Mano, D. Kojima, Y. Fukada, Pineal expression-promoting element (PIPE), a cis-acting element, directs pineal-specific gene expression in zebrafish. *Proc. Natl. Acad. Sci. U.S.A.* **99**, 15456–15461 (2002).

47. H. Mano, Y. Asaoka, D. Kojima, Y. Fukada, Brain-specific homeobox Bsx specifies identity of pineal gland between serially homologous photoreceptive organs in zebrafish. *Commun. Biol.* **2**, 364 (2019).

48. M. Takechi, T. Hamaoka, S. Kawamura, Fluorescence visualization of ultraviolet-sensitive cone photoreceptor development in living zebrafish. *FEBS Lett.* **553**, 90–94 (2003).

49. T. Tsujimura, A. Chinen, S. Kawamura, Identification of a locus control region for quadruplicated green-sensitive opsin genes in zebrafish. *Proc. Natl. Acad. Sci. U.S.A.* **104**, 12813–12818 (2007).

50. T. Tsujimura, T. Hosoya, S. Kawamura, A single enhancer regulating the differential expression of duplicated red-sensitive opsin genes in zebrafish. *PLOS Genet.* **6**, e1001245 (2010).

51. J. A. Gagnon, E. Valen, S. B. Thyme, P. Huang, L. Ahkmetova, A. Pauli, T. G. Montague, S. Zimmerman, C. Richter, A. F. Schier, Efficient mutagenesis by Cas9 protein-mediated

oligonucleotide insertion and large-scale assessment of single-guide RNAs. *PLOS ONE* **9**, e98186 (2014).

52. L.-E. Jao, S. R. Wente, W. Chen, Efficient multiplex biallelic zebrafish genome editing using a CRISPR nuclease system. *Proc. Natl. Acad. Sci.* **110**, 13904–13909 (2013).

53. S. Ansai, M. Kinoshita, Targeted mutagenesis using CRISPR/Cas system in medaka. *Biol. Open.* **3**, 362–371 (2014).

54. S. Ota, Y. Hisano, M. Muraki, K. Hoshijima, T. J. Dahlem, D. J. Grunwald, Y. Okada, A. Kawahara, Efficient identification of TALEN-mediated genome modifications using heteroduplex mobility assays. *Genes Cells* **18**, 450–458 (2013).

55. H. M. T. Choi, M. Schwarzkopf, M. E. Fornace, A. Acharya, G. Artavanis, J. Stegmaier, A. Cunha, N. A. Pierce, Third-generation in situ hybridization chain reaction: Multiplexed, quantitative, sensitive, versatile, robust. *Development* **145**, dev165753 (2018).

56. K. Kawakami, H. Takeda, N. Kawakami, M. Kobayashi, N. Matsuda, M. Mishina, A transposon-mediated gene trap approach identifies developmentally regulated genes in zebrafish. *Dev. Cell* **7**, 133–144 (2004).

57. J. C. Corbo, K. A. Lawrence, M. Karlstetter, C. A. Myers, M. Abdelaziz, W. Dirkes, K. Weigelt, M. Seifert, V. Benes, L. G. Fritsche, B. H. F. Weber, T. Langmann, CRX ChIP-seq reveals the cis-regulatory architecture of mouse photoreceptors. *Genome Res.* **20**, 1512–1525 (2010).

58. G. Badis, M. F. Berger, A. A. Philippakis, S. Talukder, A. R. Gehrke, S. A. Jaeger, E. T. Chan, G. Metzler, A. Vedenko, X. Chen, H. Kuznetsov, C.-F. Wang, D. Coburn, D. E. Newburger, Q. Morris, T. R. Hughes, M. L. Bulyk, Diversity and complexity in DNA recognition by transcription factors. *Science* **324**, 1720–1723 (2009).

59. T. L. Bailey, M. Boden, F. A. Buske, M. Frith, C. E. Grant, L. Clementi, J. Ren, W. W. Li, W. S. Noble, MEME Suite: Tools for motif discovery and searching. *Nucleic Acids Res.* **37**, 202–208 (2009).

60. K. Katoh, D. M. Standley, MAFFT multiple sequence alignment software version 7: Improvements in performance and usability. *Mol. Biol. Evol.* **30**, 772–780 (2013).

61. A. M. Kozlov, D. Darriba, T. Flouri, B. Morel, A. Stamatakis, J. Wren, RAxML-NG: A fast, scalable and user-friendly tool for maximum likelihood phylogenetic inference. *Bioinformatics* **35**, 4453–4455 (2019).

62. D. Darriba, D. Posada, A. M. Kozlov, A. Stamatakis, B. Morel, T. Flouri, ModelTest-NG: A new and scalable tool for the selection of DNA and protein evolutionary models. *Mol. Biol. Evol.* **37**, 291–294 (2020).

63. J. Li, A. C. Dantas Machado, M. Guo, J. M. Sagendorf, Z. Zhou, L. Jiang, X. Chen, D. Wu, L. Qu, Z. Chen, L. Chen, R. Rohs, Y. Chen, Structure of the forkhead domain of FOXA2 bound to a complete DNA consensus site. *Biochemistry* **56**, 3745–3753 (2017).

64. D. Lagman, D. Ocampo Daza, J. Widmark, X. M. Abalo, G. Sundström, D. Larhammar, The vertebrate ancestral repertoire of visual opsins, transducin alpha subunits and oxytocin/vasopressin receptors was established by duplication of their shared genomic region in the two rounds of early vertebrate genome duplications. *BMC Evol. Biol.* **13**, 238 (2013).

65. T. Yoshizawa, Y. Shichida, Y. Fukada, Biochemical and photochemical analyses of retinal proteins in chicken cone cells. *Pure Appl. Chem.* **63**, 171–176 (1991).

66. G. B. Gillard, L. Grønvold, L. L. Røsæg, M. M. Holen, Ø. Monsen, B. F. Koop, E. B. Rondeau, M. K. Gundappa, J. Mendoza, D. J. Macqueen, R. V. Rohlfs, S. R. Sandve, T. R. Hvidsten, Comparative regulomics supports pervasive selection on gene dosage following whole genome duplication. *Genome Biol.* **22**, 103 (2021).